Design and CFD Analysis of Hypersonic Nose Cone

Naveen Kumar G[1], Dr. Velliangiri M[2], Kamesh Adithya S B[3], Kirubakaran A[4], Kishore M[5]

[1, 3, 4, 5]Undergraduate students, [2]Assistant professor, Department of Mechanical Engineering, Coimbatore Institute of Technology, Coimbatore – 641014, Tamil Nadu, India

Abstract: Nose cone comprises the most significant component while designing high speed aircrafts. The objects moving at high speeds encounter forces which tend to decelerate the objects. The resistance that is set up in the medium is known as drag and it is concerned while designing high speed aircrafts. Nose cones of power series 0.6 and 0.75 are studied with respect to different Mach numbers over a range 1 - 12 and analyzed using CFD analysis. The drag and stagnation properties of nose cones are compared between them and with analytically calculated calculations. The aim of the paper is designing a hypersonic nose cone with minimum air drag values and to predict those values.
Keywords: Drag, Mach number, power series, stagnation properties

I. INTRODUCTION

In the present scenario of rocket science, there is a need and urge for the development of hypersonic aircrafts. Hypersonic aircrafts can travel much faster than current nuclear-capable ballistic and cruise missiles at low altitudes, can switch direction in flight and do not follow a predictable arc like conventional missiles, making them much harder to track and intercept. Brahmos II is a hypersonic cruise missile currently under joint development by Russia's NPO Mashinostroyenia and India's Defense, which have together formed Brahmos Aerospace Private Limited. A nose cone is the forward most section of a rocket, guided missile or aircraft. The cone is shaped to minimize aerodynamic drag. Nose cones are also designed for travel in and under water and in high-speed land vehicles. There is a need for development of hypersonic nose cone in the future to come.

II. METHODOLOGY

The sequence of works carried out is depicted in the following flowchart which clearly indicates the methodology that is been followed.
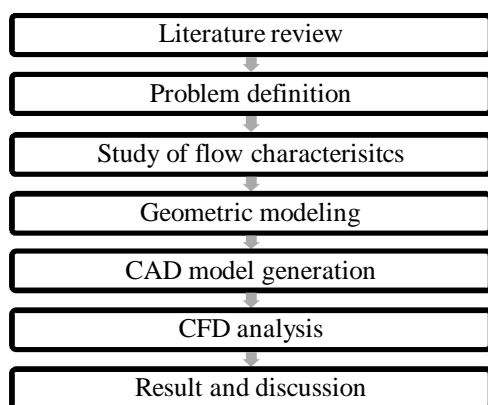

Fig. 1 Methodology

III. LITERATURE REVIEW

Kaleeswaran et al. (2013) proposed the aerodynamic study over 2D supersonic nose cone models of missiles. First a spherical nose cone model was tested with a mach number of 3 and then with the same Mach speed another Spherical model with a parabolic nose cavity was tested. Both the models were designed in GAMBIT and analysed in FLUENT. The authors concluded that the supersonic region is associated with the shock waves mostly moving downstream. High temperature, pressure regions were found to appear in front of nose. This in turn reduces the surfaces pressure effects and in turn reducing wave and aerodynamic drag to a great extend.
Narayan et al. (2017) proposed a comparative study of the hypersonic flow past spherically blunted and parabolic nose cones at a Mach number of 5.8, numerically. Studies on spherically blunted and parabolic nose cones are performed for different fineness

ratios at zero angle of attack. The authors investigated the flow/shock features in the vicinity of the blunted and parabolic nose cones for different fineness ratios is also shown in order to determine its influence on aerodynamic drag. The authors concluded that parabolic nose cones at higher fineness ratios are preferred over spherically blunted ones for achieving higher drag reductions and lower heating in hypervelocity vehicles. Li et al. (2013) investigated on how the shape of the nose cone has a significant effect on the drag of the vehicle. The author's conceptualization is proposing morphing nose cone to reduce the drag when the re entry vehicle flies back into the atmosphere. The morphine nose cone has deformable shape in different flight phases. The authors concluded that the spherical cap is non deformable where the curvature of the deformable ogive is varied with the changes of aerodynamic load. Varma (2016) investigated various nose profiles and compared it to know performance over existing conventional nose profiles. The author proposed to identify the types of nose profiles and its specific aerodynamic characteristics with minimum pressure coefficient and critical Mach number. CFD analysis is carried out using ANSYS for different profiles of nose like cone, parabola, ogive and Von Karman ogive with a fitness ratio of 6 to improve aerodynamic characteristics of missile or rocket in subsonic conditions. The author concluded that the Von Karman ogive nose profile gives higher critical Mach.

Author, C. (2018) proposed that the objects moving at high speeds encounter forces which tend to decelerate the objects. This resistance in the medium is termed as drag which is one of the major concerns while designing high speed aircrafts. The author encountered another key factor which influences the design is the air drag. The main challenge faced by aerospace industries is to design the shape nose of the flying object that travels at high speeds with optimum values of air drag. The author investigated the subsonic flow considering various shapes of nose cone profiles.

IV. FACTORS AND ASSUMPTIONS

The sequence of works carried out is depicted in the following flowchart which clearly indicates the methodology that is been followed.

A. Factors affecting drag
The drag force is defined as,

$$F_d = \frac{C_d \rho u^2 A}{2}$$

The factors affecting drag are explained as follows:

1) *Area of an object:* Drag increases with area. Area refers to the area of contact between the object and the fluid. Surface area is not important while dealing with pressure drag, but it is important when dealing with viscous drag. More surface area means more of the object is in contact with the fluid, which means more drag.

2) *Size and shape of an object:* Geometry has a large effect on the amount of drag generated by an object. As with lift, the drag depends linearly on the size of the object moving through the air. The cross-sectional shape of an object determines the form drag created by the pressure variation around the object.

3) *Surface finish of an object:* Drag is a form of aerodynamic friction. The amount of drag depends on the surface roughness of the object; a smooth, waxed surface produces less drag than a roughened surface. This effect is called skin friction and is usually included in the measured drag coefficient of the object.

4) *Density of air:* Drag increases with the density of the fluid. With increase in density, mass and inertia increase which in turn increases the resistance to flow. Thus the two quantities are directly proportional.

5) *Viscosity of air:* If the viscosity of the fluid increases, it means the surrounding temperature is gradually dropping. Temperature is the function of viscosity. The lower the temperature, the higher is the viscosity. So the drag coefficient increases with the increase in viscosity.

6) *Compressibility of air:* The drag also depends in a complex way on the compressibility of air. The viscosity and compressibility of air affect the wave drag and skin friction to a large extent.

7) *Velocity:* Drag is associated with the movement of the aircraft through the air, so drag depends on the velocity of the air. Like lift, drag actually varies with the square of the relative velocity between the object and the air.

8) *The body's inclination to the flow:* The inclination of the object to the flow also affects the amount of drag generated by a given shaped object. If the object moves through the air at speeds near the speed of sound, shock waves are formed on the object which create an additional drag component called wave drag.

9) *Boundary layer separation:* The motion of the object through the air also causes boundary layers to form on the object. A boundary layer is a region of very low speed flow near the surface which contributes to the skin friction.

B. Assumptions considered

The assumptions are explained clearly as follows,

1) *Fineness ratio (FR):* The ratio of the length of a nose cone compared to its base diameter is known as the fineness ratio. This is sometimes also called as aspect ratio. The fineness ratio is assumed to be 5:1 as per literature review made; this ratio is found to be optimal.

2) *Altitude:* Altitude is the vertical distance of the aircraft above the terrain over which it is flying. The maximum altitude up to which the aircraft flies is assumed to be 10,000 meters.

3) *Flow medium:* The Medium of flow is assumed to be air.

4) *Angle of attack: Angle of attack* (AOA) is the *angle* between the oncoming air or relative wind and a reference line on the *airplane* or wing. It can also be defined as the angle between a reference line on a body and the vector representing the relative motion between the body and the fluid through which it is moving. The angle of attack is assumed to be zero.

5) *Wind conditions:* The state of wind varies from place to place. The speed, direction and certain other properties of wind are subjected to change with place and time. It is a factor which is not considered in study. The wind conditions are assumed to be stable and are considered as independent variables.

6) *Temperature:* Atmospheric temperature is a measure of temperature at different levels of the Earth's atmosphere. It is governed by many factors, including incoming solar radiation, humidity and altitude. The temperature is assumed to be stable and is considered as an independent variable.

7) *Surface finish:* Surface finish, also known as surface texture is the nature of a surface as defined by the three characteristics of lay, surface roughness, and waviness. The surface finish of the wetted area exposed to air flow is assumed to be constant.

8) *Roll:* An aircraft in flight is free to rotate in three dimensions. Roll is defined as the rotation about an axis running from nose to tail. It is assumed that there is no roll during flight.

9) *Aerodynamic heating effect:* Aerodynamic heating is the heating of a solid body produced by its high-speed passage through air (or by the passage of air past a static body), whereby its kinetic energy is converted to heat by adiabatic heating, and by skin friction on the surface of the object at a rate that depends on the viscosity and speed of the air. It is assumed that there is no roll during flight.

V. DESIGN METHODOLOGY

The design of hypersonic nose cone has dealt with by following certain sequence of works which is depicted in the following flowchart.
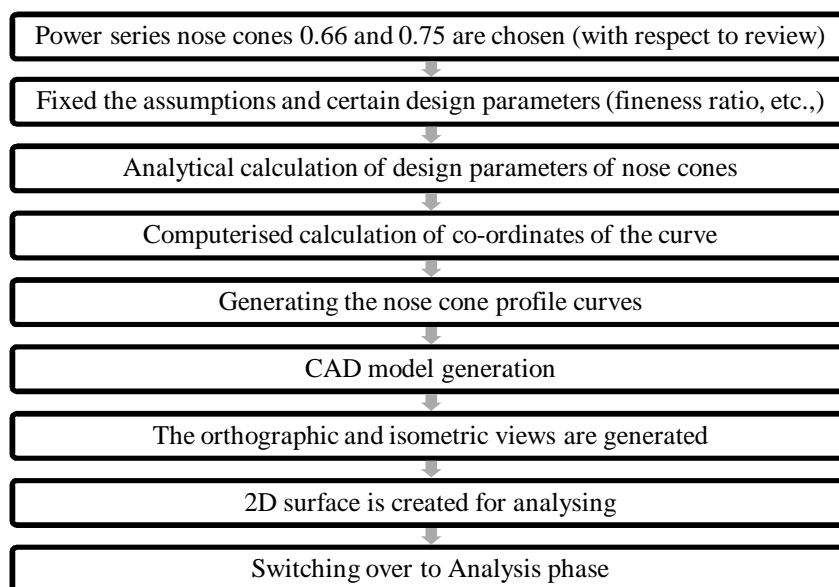
```
┌──────────────────────────────────────────────────────────────────┐
│ Power series nose cones 0.66 and 0.75 are chosen (with respect to review) │
└──────────────────────────────────────────────────────────────────┘
                                    ↓
┌──────────────────────────────────────────────────────────────────┐
│ Fixed the assumptions and certain design parameters (fineness ratio, etc.,) │
└──────────────────────────────────────────────────────────────────┘
                                    ↓
┌──────────────────────────────────────────────────────────────────┐
│ Analytical calculation of design parameters of nose cones │
└──────────────────────────────────────────────────────────────────┘
                                    ↓
┌──────────────────────────────────────────────────────────────────┐
│ Computerised calculation of co-ordinates of the curve │
└──────────────────────────────────────────────────────────────────┘
                                    ↓
┌──────────────────────────────────────────────────────────────────┐
│ Generating the nose cone profile curves │
└──────────────────────────────────────────────────────────────────┘
                                    ↓
┌──────────────────────────────────────────────────────────────────┐
│ CAD model generation │
└──────────────────────────────────────────────────────────────────┘
                                    ↓
┌──────────────────────────────────────────────────────────────────┐
│ The orthographic and isometric views are generated │
└──────────────────────────────────────────────────────────────────┘
                                    ↓
┌──────────────────────────────────────────────────────────────────┐
│ 2D surface is created for analysing │
└──────────────────────────────────────────────────────────────────┘
                                    ↓
┌──────────────────────────────────────────────────────────────────┐
│ Switching over to Analysis phase │
└──────────────────────────────────────────────────────────────────┘
```

Fig. 2 Design methodology

VI. GEOMETRICAL MODELLING

The nose cone profiles chosen for designing and analysis in hypersonic conditions are

1) Power series nose cone with n = 0.66
2) Power series nose cone with n = 0.75

The above nose cone profiles are chosen with respect to the literature review made. It is evident from literature review that these nose cone profiles have minimum drag coefficient when compared to other nose cones at hypersonic conditions. The geometrical modelling is carried out after assuming certain conditions which are clearly mentioned in the preceding section. The fineness ratio is chosen to be 5:1. The diameter of the nose cone is considered to be 0.6 metres such that the length of the nose cone is 3 metres.

The power series nose cone is defined in terms of L and n as follows:

For $0 \leq n \leq 1$:

$$y = R \left(\frac{x}{L}\right)^n$$

-   Where n is chosen to be 0.66 and 0.75

Based on the values of chosen n, length and radius of nose cone profiles, a table between the horizontal and vertical co-ordinates of the nose cone profiles is created. The precision of nose cone profiles is fixed to be 0.5 millimetres. The range of horizontal co-ordinate is from 0 to 3 meters (the overall length of nose cone) in the order of 0.5 millimetres. The vertical co-ordinate with respect to different horizontal co-ordinate is calculated and tabulated. The calculation is mathematically correct if the vertical co-ordinate, y turns out to be 0.3 meters (radius of nose cone) at horizontal co-ordinate, x = L = 3 meters.

A curve is created between the horizontal and vertical co-ordinates which give the profile of nose cone to be traced. The tabulation is stored in .txt (Bitmap text) format such that it can be imported into a CAD modelling platform. The nose cone profile that is to be imported is stored in .txt format. It is then imported into CAD platform and the 2D surface is generated for carrying out analysis.
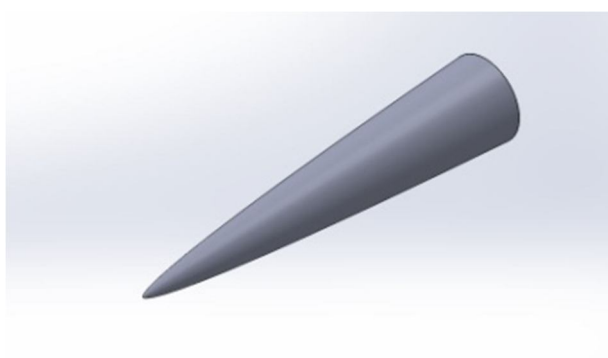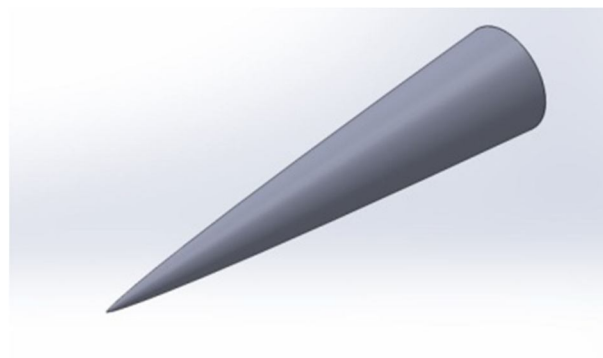
| (A) Nose cone n = 0.66 | (B) Nose cone n = 0.75 |

Fig. 3 Isometric views of nose cones
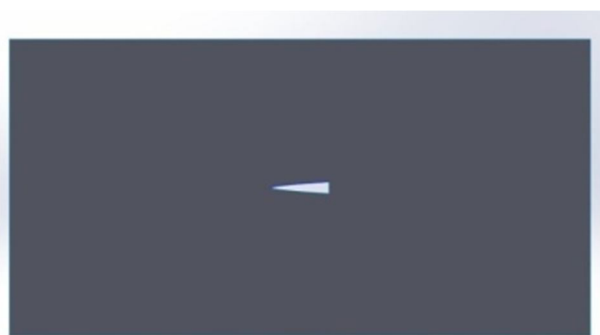
| (A) Nose cone n = 0.66 | (B) Nose cone n = 0.75 |

Fig. 4 Surface of nose cones for analysis

VII.   GRID GENERATION

After importing the CAD model, meshing or grid generation is carried out. The type of mesh is triangular mesh. After face meshing and body sizing at the mesh part coordinate name was selected along the boundary named: Inlet, outlet and walls. The number of elements and nodes formed for power series no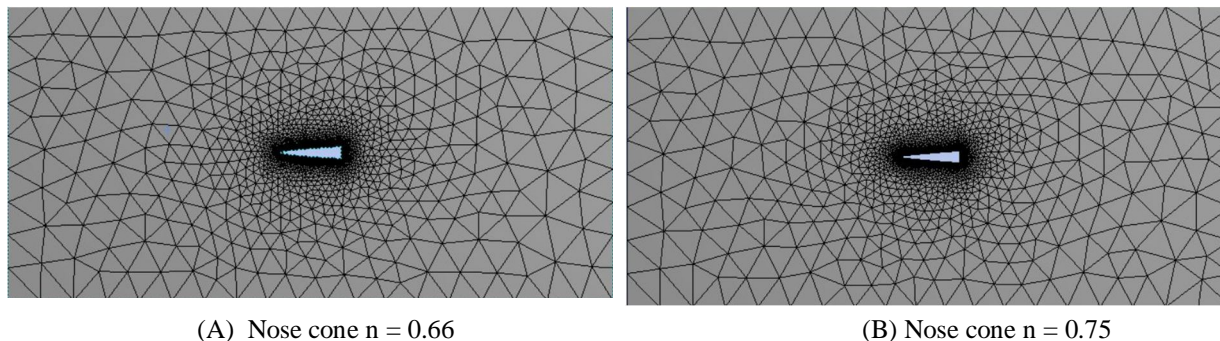se cone 0.66 are 11630 elements and 6221 nodes respectively. The number of elements and nodes formed for power series nose cone 0.75 are 9653 elements and 5159 nodes respectively.

(A) Nose cone n = 0.66   (B) Nose cone n = 0.75

Fig. 5 Mesh pattern

VIII.   PRE PROCESSING

The pre processing process involves definition of fluid properties since every fluid domain or surface has its own distinct property. The boundary conditions are also mentioned since each unique setup of the CFD domain must have an initialization, and it is fulfilled by the boundary conditions input. Specification of appropriate boundary conditions at cells is required which coincides with the domain boundary.

The pre processing procedure of hypersonic nose cone is depicted in the following flowchart.
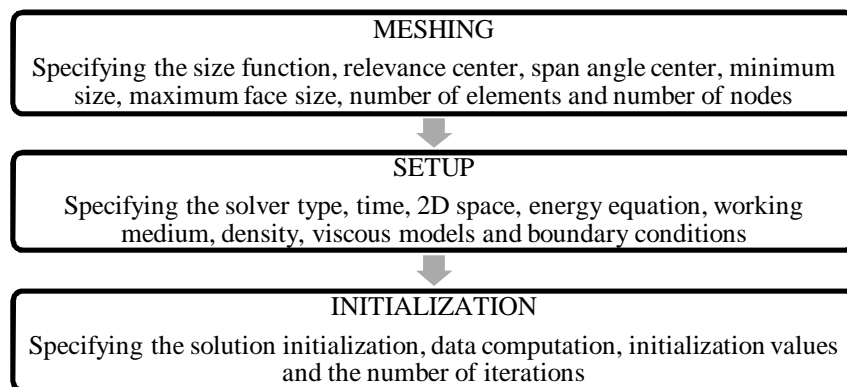
Fig. 6 Pre processing procedure

At the setup portion Solver type was selected as density based, time was steady and 2D space was selected as Planar. Then in model section energy equation was on and viscous model is chosen. Air is taken as a working medium and density was selected as an ideal gas. The type of viscous models chosen for carrying out CFD analysis of nose cones is SST k-omega. The Mach numbers that are chosen are Mach 5 (1701.45 m/s), Mach 7 (2401 m/s), Mach 10 (3430 m/s) and Mach 12 (4116 m/s).

At boundary condition section, velocity inlet is chosen and the velocity at inlet is given in the order of Mach numbers of 5, 7, 10 and 12 (1701.45, 2401, 3430, 4116 m/s respectively). The initial gauge pressure at the inlet was given as 26436.23 Pa; the total temperature at the inlet was given as 223 K. The pressure outlet is chosen; the gauge pressure at the outlet was given as 0 Pa, the backflow total temperature was given as 300 K.

Fluent defines the total pressure as gauge pressure with respect to operating pressure. It also defines the total temperature as a gauge temperature with respect to operating temperature. Standard initialization was selected as solution initialization and the data was computed from the velocity inlet. The gauge pressure was given as 26436.23 Pa; the temperature was given as 223 K. The velocity in x - direction was given as 1701.45/ 2401/ 3430/ 4116 m/s. The velocity in y - direction was given as 0 m/s. The calculation is carried out for 1500, 2000 iterations for power series nose cones of 0.66, 0.75 respectively. The analysis setup and iijitialization values of nose cone are as follows.

TABLE I

Analysis Setup and Initialization Values of Nose Cones

S. No	MESHING	
1.	Size function	Curvature
2.	Relevance center	Fine
3.	Span angle center	Fine
4.	Minimum size	1 mm
5.	Maximum face size	Default
6.	Number of elements	Power series nose cone 0.66: 11630; Power series nose cone 0.75: 6221
7.	Number of nodes	Power series nose cone 0.66: 9653; Power series nose cone 0.75: 5159
S. No	**SETUP**	
1.	Solver type	Density based
2.	Time	Steady
3.	2D space	Planar
4.	Energy equation	On
5.	Working medium	Air
6.	Density	As that of ideal gas
7.	Viscous models	SST k-omega
8.	Boundary conditions	Inlet conditions: ✓ Velocity inlet is chosen ✓ Velocity: Mach 5, 7, 10, 12 ✓ Inlet gauge pressure: 26436.23 Pa ✓ Inlet total temperature: 223 K Outlet conditions: ✓ Pressure outlet is chosen ✓ Outlet gauge pressure: 0 Pa ✓ Backflow total temperature: 300 K
S. No	**INITIALIZATION**	
1.	Solution initialization	Standard initialization
2.	Data computation	From Velocity inlet
3.	Initialization values	✓ Gauge pressure: 26436.23 Pa ✓ Gauge temperature: 223 K ✓ Velocity (x - direction): Mach 5, 7, 10, 12 ✓ Velocity (y - direction): 0 m/s
4.	Number of iterations	Power series nose cone 0.66: 1500 iterations Power series nose cone 0.75: 2000 iterations

IX. RESULTS AND DISCUSSIONS

The results are extracted from CFD POST after the analysis from fluent flow solver. The velocity, pressure and temperature contours of chosen nose cone profiles with respect to varying Mach numbers are displayed below.

The velocity contours of power series nose cones of 0.66 and 0.75 with respect to varying Mach numbers are displayed below.
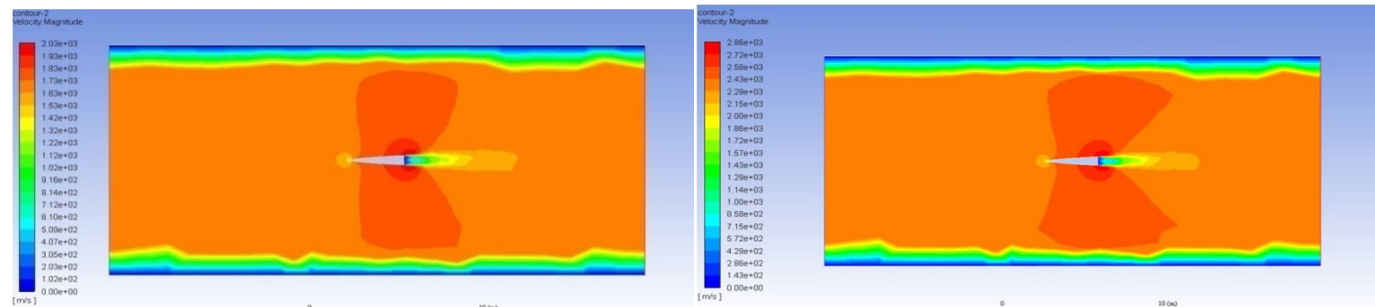
7.1 (A) Mach = 5

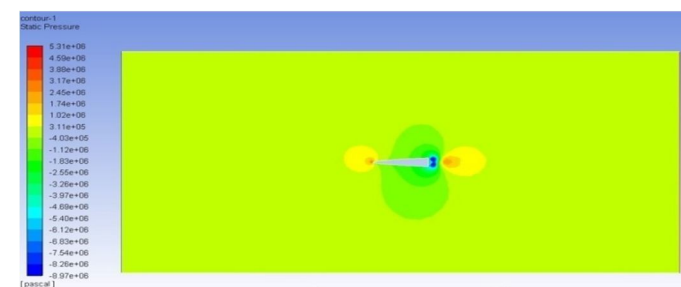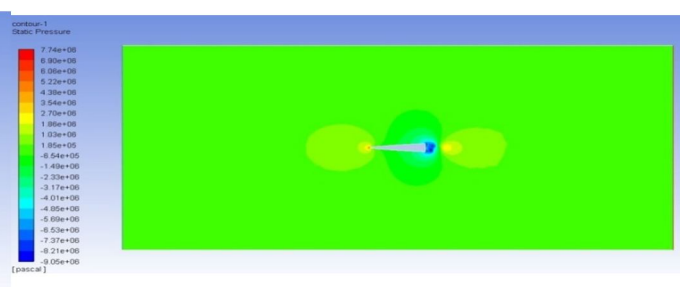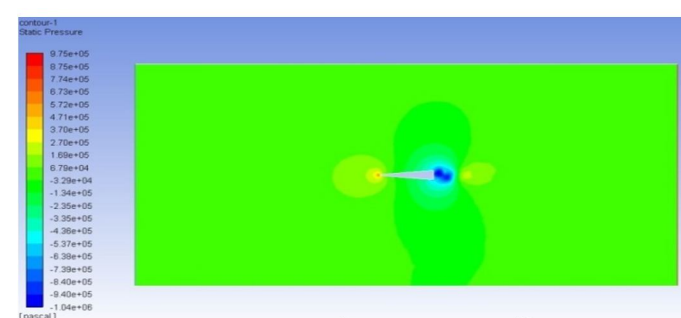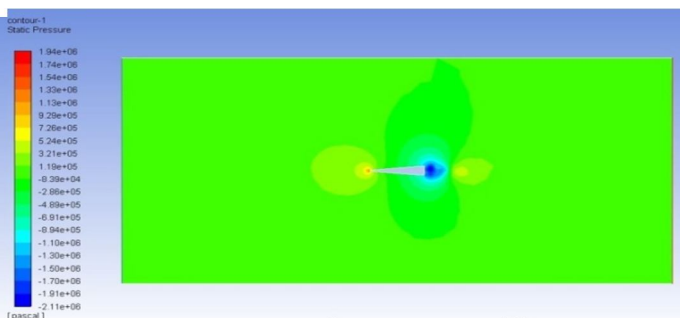7.1 (B) Mach = 7
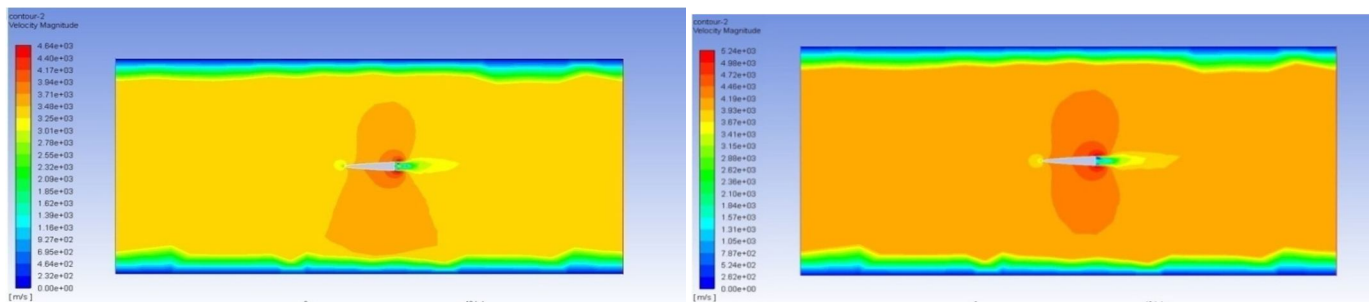
7.1 (C) Mach = 10

7.1 (D) Mach = 12
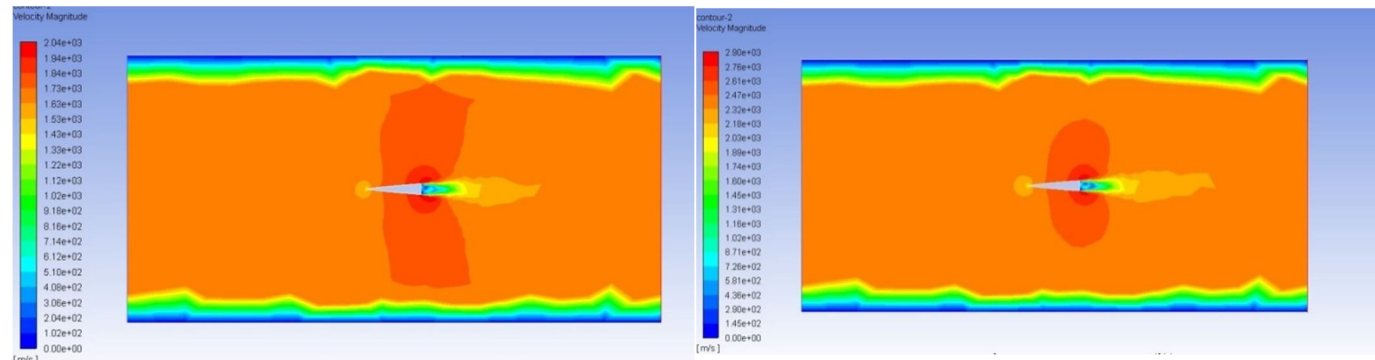
7.2 (A) Mach = 5

7.2 (B) Mach = 7
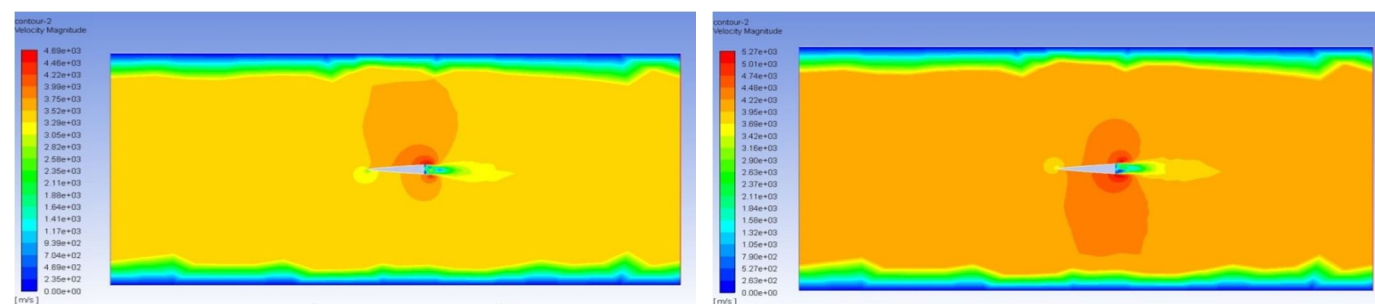
7.2 (C) Mach = 10

7.2 (D) Mach = 12

7.1 Power series nose cone n = 0.66

7.2 Power series nose cone n = 0.75

Fig.7 Velocity Contours of Nose Cones

The velocity contours are obtained by simulating power series nose cones 0.66 and 0.75 in SST k - omega viscous model. High velocity concentration acts on the tip of the nose cones (As per simulation the contour is concentrated on the backend of nose due to sudden geometrical change. It is not considered here since on practical aspect, there will be no such sudden change in geometry). Upon observation, it is evident that the velocity concentration region about the nose tip is higher for power series nose cone 0.75 as compared to that of nose cone 0.66. Also it is observed that the amount of area of velocity distribution is large as in case of nose cone 0.75 than that of nose cone 0.66.

The pressure contours of power series nose cones of 0.66 and 0.75 with respect to varying Mach numbers are as follows.
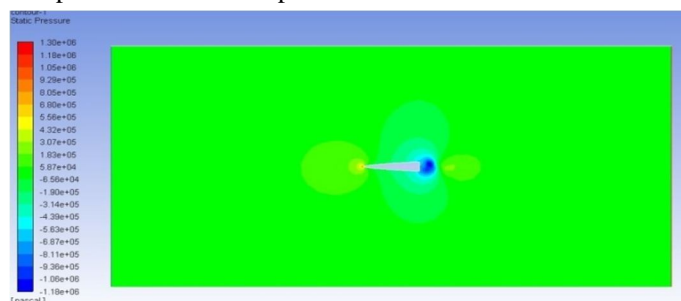
8.1 (A) Mach = 5
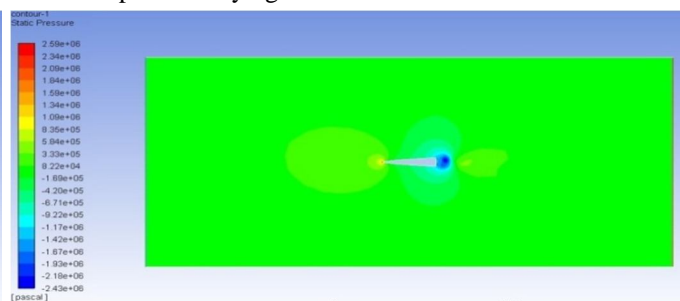
8.1 (B) Mach = 7

8.1 (C) Mach = 10

8.1 (D) Mach = 12

8.2 (A) Mach = 5

8.2 (B) Mach = 7
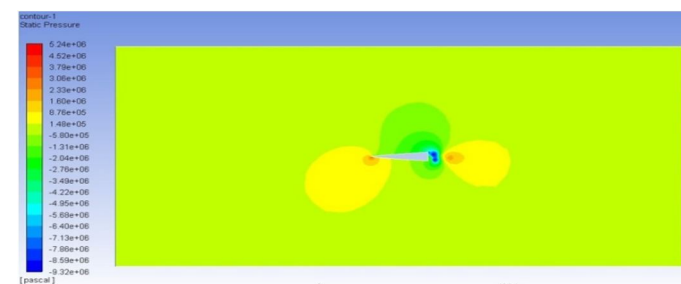
8.2 (C) Mach = 10
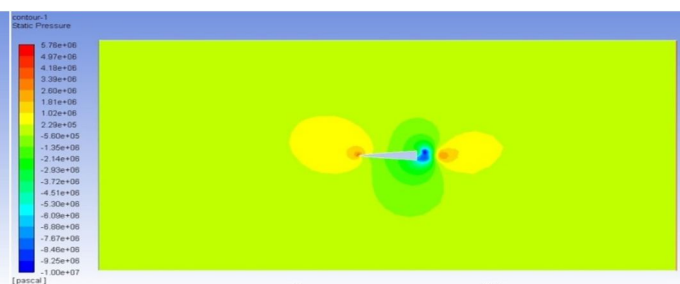
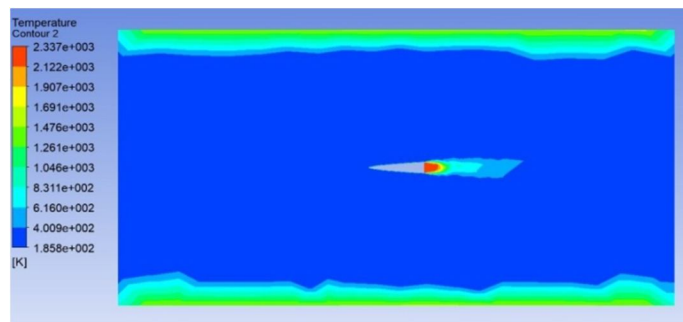8.2 (D) Mach = 12

8.1 Power series nose cone n = 0.66

8.2 Power series nose cone n = 0.75

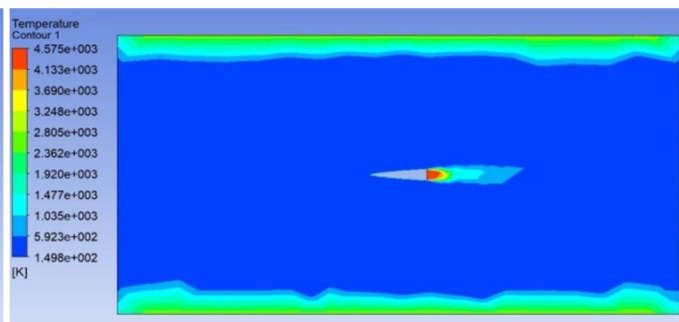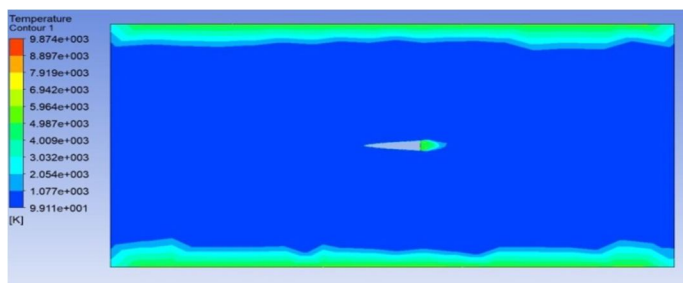Fig.8 Pressure Contours of Nose Cones

High pressure concentration acts on the tip of the nose cones. There is a region or cloud of low pressure concentration at the rear portion of nose cones due to sudden geometrical change (Not considered here for practical reasons).

Upon observation, it is evident that the stagnation pressure of power series nose cone 0.66 is nearer to analytically calculated values as compared to that of nose cone 0.66. Also it is observed that the pressure distribution zone is uneven in nose cone 0.66 when compared to nose cone 0.66.

The temperature contours of power series nose cones of 0.66 and 0.75 with respect to varying Mach numbers are displayed below.
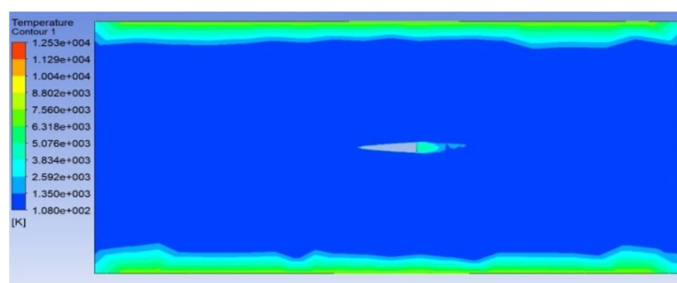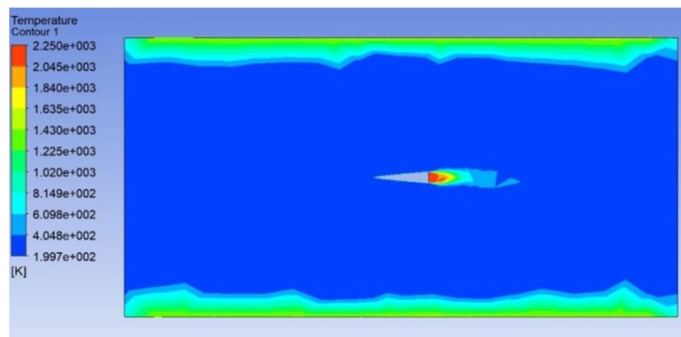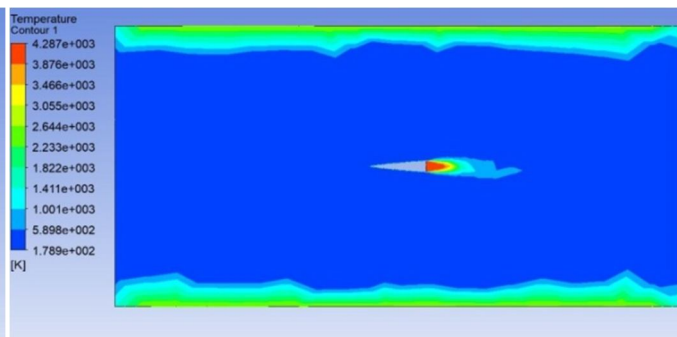

9.1 (A) Mach = 5

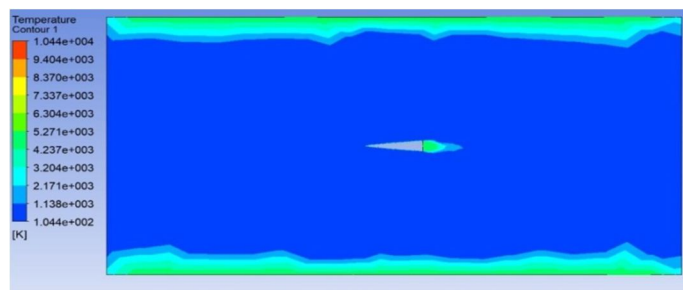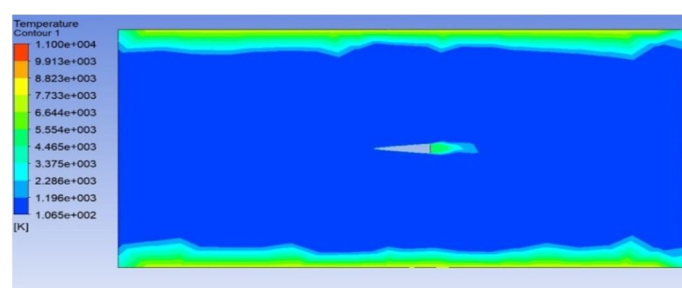9.1 (B) Mach = 7

9.1 (C) Mach = 10

9.1 (D) Mach = 12

9.2 (A) Mach = 5

9.2 (B) Mach = 7

9.2 (C) Mach = 10

9.2 (D) Mach = 12

9.1 Power series nose cone n = 0.66

9.2 Power series nose cone n = 0.75

Fig.9 Temperature Contours of Nose Cones

The temperature contours are obtained by simulating power series nose cones 0.66 and 0.75 in SST k - omega viscous model. High temperature concentration acts on the tip of the nose cones (As per simulation the contour is concentrated on the backend of nose due to sudden geometrical change (Not considered here for practical reasons).

Upon observation, it is evident that the temperature concentration region about the nose tip is higher for power series nose cone 0.75 as compared to that of nose cone 0.66.

Also it is observed that the as the velocity increases, the temperature gradually distribute from the nose tip along the body of the nose cone.

The stagnation properties obtained as a result of simulating chosen nose cone profiles in SST k - omega viscous model is found to be lesser than that of analytically calculated stagnation properties values.

The stagnation properties obtained as a result of simulating chosen nose cone profiles in SST k - omega viscous model and analytical calculations are mentioned in the form of table below.

TABLE III
Comparison of Stagnation properties of specified Mach number with proximity to the calculated stagnation properties' values
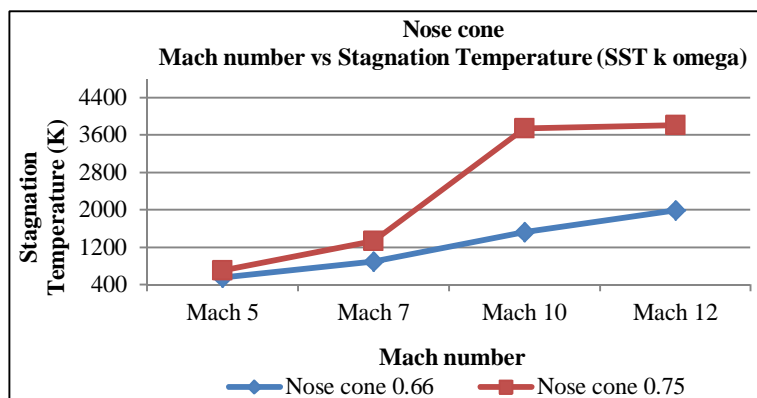
Mach number	Stagnation Properties					
	Stagnation pressure (e+06 Pa)			Stagnation temperature (e+03 K)		
	Analytical calculation	Simulation (SST k omega)		Analytical calculation	Simulation (SST k omega)	
		Power series Nose cone			Power series Nose cone	
		n = 0.66	n = 0.75		n = 0.66	n = 0.75
M = 5	13.96	1.275	0.975	1.336	0.555	0.708
M = 7	109.09	2.59	1.94	2.399	0.896	1.327
M = 10	1118.64	5.31	5.24	4.747	1.521	3.742
M = 12	4330.64	7.74	5.76	7.636	1.986	3.803

Based upon the calculations made and with respect to the above mentioned table, it is found that the stagnation temperature (the most important result of drag) is higher for nose cone of 0.75 when compared to that of nose cone 0.66. Hence, based upon the stagnation results, nose cone 0.66 can be chosen.

The stagnation properties obtained as a result of simulating chosen nose cone profiles 0.66 and 0.75 in SST k - omega viscous model are mentioned in the form of graphical representations below. It is done so as to achieve a visually viable result and conclusion on which nose cone profile to choose.
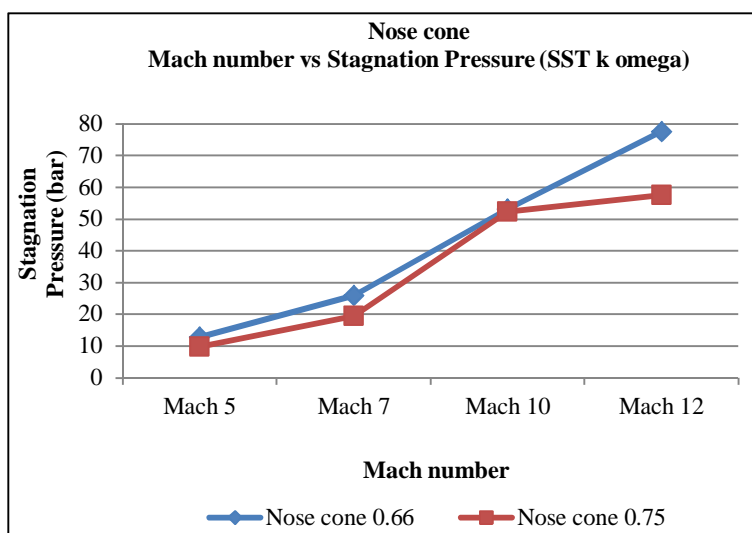
(A) Mach number vs Stagnation pressure

(B) Mach number vs Stagnation temperature

Fig. 10 Variation of stagnation properties of nose cones

Based on the Mach number vs Stagnation Pressure graph, it is evident that the stagnation pressure changes abruptly for nose cone of n = 0.75 and gradually for nose cone 0.66. At hypersonic speeds, it is found that the stagnation pressure of nose cone 0.75 is lesser than that of nose cone 0.66. Based on the Mach number vs Stagnation temperature graph, it is evident that the stagnation temperature changes abruptly for nose cone of n = 0.75 and for nose cone 0.66 it is gradual.

Stagnation temperature is the main factor increasing the drag of nose cone. Here, it is evident that nose cone 0.66 has lesser stagnation temperature than that of nose cone 0.75.

TABLE IIIII
Comparison of drag characteristics of nose cones

Mach number	Drag characteristics			
	Drag force (N)		Coefficient of drag	
	Power series nose cone		Power series nose cone	
	n = 0.66	n = 0.75	n = 0.66	n = 0.75
	Simulation (SST k omega)			
M = 5	261592.12	334700.63	0.147529	0.188760
M = 7	518347.16	621620.87	0.146792	0.176054
M = 10	1079943.88	1193938.7	0.149868	0.165682
M = 12	1785462.3	1844593.9	0.172065	0.177757

The drag characteristics obtained as a result of simulating chosen nose cone profiles in SST k - omega viscous model is found to be lesser. Hence, it is found that the chosen nose cone profiles are efficient and provide less aerodynamic resistance. The drag force and coefficient of drag obtained as a result of simulating chosen nose cone profiles in SST k - omega viscous model are mentioned in the form of table above. It is evident that drag force and coefficient of drag of nose cone 0.66 is lesser than that of nose cone 0.75. The variation of drag force of chosen nose cone profiles with respect to varying Mach numbers is depicted in the form of graphical representation below.
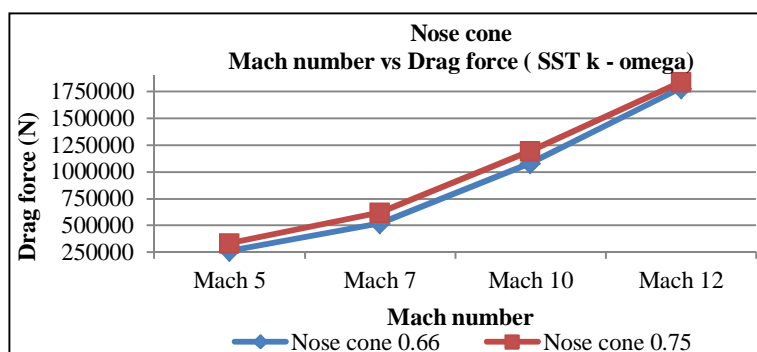
(A) Mach number vs Drag force
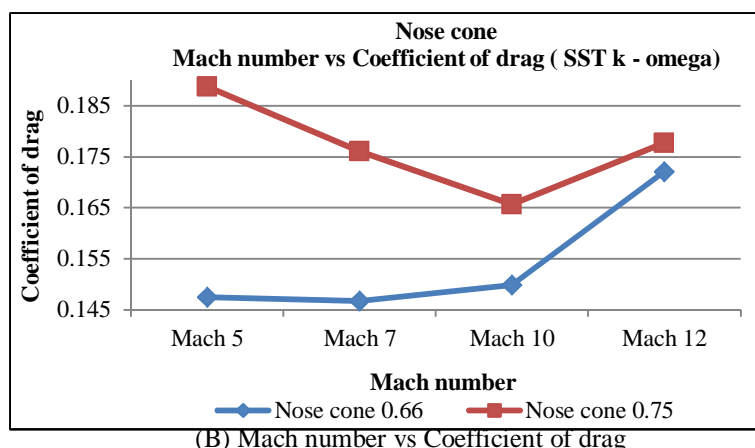
(B) Mach number vs Coefficient of drag
Fig.11 Variation of drag characteristics of nose cones

Based on the Mach number vs Drag force graph, it is evident that the drag force for nose cone 0.66 is lesser than that of nose cone 0.75. Based on the Mach number vs Coefficient of drag graph, it is evident that the coefficient of drag changes abruptly for nose cone 0.75 while it is gradually increasing for nose cone 0.66. The coefficient of drag is found to be lesser for nose cone 0.66 when compared to that of nose cone 0.75.

X. CONCLUSIONS

The paper's ultimate aim is designing of hypersonic nose cone with optimum values of air drag. Based upon the results obtained, it is found that Power series nose cone of n = 0.66 is found to be efficient in hypersonic conditions with respect to the assumptions made. It is also found that the aerodynamic drag of power series nose cone 0.66 is minimal and the stagnation properties are in accordance with the analytical calculations made. Hence, at hypersonic conditions, Power series nose cone (n = 0.66) is preferred.

XI. NOMENCLATURE

TABLE IVV
SYMBOLS, ABBREVIATIONS AND NOMENCLATURE

SYMBOLS, ABBREVIATIONS AND NOMENCLATURE	CONTENT
u	Velocity (m/s)
ρ	Density (kg/m^3)
A	Area (m^2)
CFD	Computational Fluid Dynamics
3D	Three Dimension
2D	Two Dimension
CAD	Computer Aided Design
M	Mach Number
L	Length of nose cone (m)
R	Radius of nose cone (m)
x, y	Horizontal and vertical co-ordinates of nose cone
n	Power series value of nose cone
C_d	Coefficient of drag
F_d	Drag force (N)
FR	Fineness Ratio
AOA	Angle of Attack

XII. ACKNOWLEDGMENT

REFERENCES

[1]   Anderson, J.D. (2017) 'Computational Fluid Dynamics-The basics with applications' - sixth edition.

[2]   Aust, J. (2017) 'Design And Structural Analysis Of Missile Nose Cone', Basic Appl. Sci., vol.10, no. 12, pp. 30–40.

[3]   Bogdan Alexandru, B. (2015) 'Analysis of New Aerodynamic Design of the Nose Cone Section Using CFD and SPH', Incas Bull., vol. 7, no. 2, pp. 43-52.

[4]   Chalia, S. and Kumar Bharti, M. (2016) 'Mathematical Modeling of Ogive Fore bodies and Nose Cones', Int. Res. J. Eng. Technol., pp. 744–747.

[5]   Ferziger, J.H. and Peric, M. (1991) 'Computational Methods for Fluid Dynamics' - third edition.

[6]   Guzelbey, I.H. (2018) 'A Review of Aerodynamic Shape Optimization for a Missile Method of Aerodynamic Shape Optimization Classification' ISSN: 2602-3199 vol. 4 pages 94 - 102.

[7]   Journal, A. and Basic, O.F. (2017) 'Design and Structural Analysis Of Missile Nose Cone', vol. 11, no. August, pp. 30–40.

[8]   Kaleeswaran, B., Ranjith, S.and Jeniwer, N. B. (2013) 'An Aerodynamic optimization of supersonic flow over the nose section of missiles' - ISSN: 2778-0181 vol. 2 Issue 4.

[9]   Li, J., Wu, J. and Yan, S. (2013) 'Conceptual design of deployment structure of morphing nose cone', Adv. Mech. Eng., vol. 2013.

[10] Narayan, A., Narayanan, S. and Kumar, R. (2017) 'Hypersonic flow past nose cones of different geometries: a comparative study'- 94. 003754971773305. 10.1177/0037549717733051.

[11] Reddy, M.S. and Keerthi, N. (2017) 'Design and Structural Analysis of Missile Nose Cone' ISSN: 1991-8178; EISSN: 2309-8414 pages 30 - 40.

[12] Schneider, P. S. (2008) 'Summary of Hypersonic Boundary layer transition experiments on blunt bodies with roughness' - AIAA 2008-501.

[13] Senthil, S. (2009) 'Gas Dynamics and Jet propulsion' - sixth edition.

[14] Varma, A.S. (2016) 'International Journal of Aerospace and Mechanical Engineering CFD Analysis of Various Nose Profiles International Journal of Aerospace and Mechanical Engineering', vol. 3, no. 3, pp. 26–29.

[15] Yahya, S.M. (2011) 'Gas Tables-For compressible flow calculations' - sixth edition.

[16] Yeshwanth, A. and Senthiil, P. V. (2018) 'Nose cone design and analysis of an avion' - Volume 119 No. 12 2018, 15581-15589 ISSN: 1314-3395.

[17] Zaharia, S.M. and Stefaneanu, R.I. (2017) 'Design and Manufacturing Process for a Ballistic Missile' Vol. XXI No 2(42).

INTERNATIONAL JOURNAL
FOR RESEARCH

IN APPLIED SCIENCE & ENGINEERING TECHNOLOGY

Call : 08813907089 ⊘ (24*7 Support on Whatsapp)